Fair Initial Access Design for mmWave Wireless

Suresh Srinivasan¹, Xi Yu¹, Alireza Keshavarz-Haddad², and Ehsan Aryafar¹ ¹Portland State University, Computer Science Department, Portland, OR, USA ²Shiraz University, School of Electrical and Computer Engineering, Shiraz, Iran

Abstract-Millimeter-wave (mmWave) systems use highly directional beams with narrow beamwidths to overcome the high path loss associated with their frequency bands. The use of narrow beams complicates the link establishment process as the transmitter and receiver need to search for appropriate beams before they can communicate with each other. Existing mmWave standards address the beam search process as part of the initial access (IA), and use contention based schemes that let multiple clients train their beams in the same search interval. However, there exists a severe power imbalance among competing clients' beams, as clients naturally have different orientations and are at different distances from the same access point. This beam power imbalance coupled with poor contention protocols results in poor IA fairness in dynamic systems with multiple clients. We propose a joint power control and contention adaptation protocol (coined JPOC) that addresses this unfairness problem. JPOC uses an open-loop and client-side power control mechanism that reduces the beam power imbalance among competing clients. It also uses a model-driven contention adaptation protocol that optimally adjusts the duration of the contention time according to the system dynamics. Comprehensive evaluation through a mixture of experiments and simulations show that compared to existing 802.11 ad/ay standards, JPOC substantially reduces the contention overhead and increases the IA fairness.

I. Introduction

MmWave communication is one of the essential components of next generation wireless networks to support extremely high data rate services. The mmWave frequency bands provide an order of magnitude more spectrum than already congested sub-6 GHz bands, which can be used to boost the communication capacity. However, mmWave systems suffer from high path loss, high noise power, and susceptibility to blockages such as humans¹ [2]. To address these challenges, mmWave systems use an array of antennas and form highly directional beams² at both the transmitter (Tx) and receiver (Rx) to increase the SNR. These directional beams reduce the interference, boost the capacity, and increase the security of communication³, however, the plurality of narrow beams at the Tx and Rx makes the initial access (IA) and adaptation to mobility much harder. IA is a process by which an access point (AP) and a client device establish a physical connection, after which the data communication can start. In mmWave systems, the Tx and Rx need to find appropriate beams before they can communicate.

This beam training procedure in the existing standards (e.g., 3GPP 5G and IEEE 802.11 ad/ay) is handled during the IA.

A. Related Work

In IEEE 802.11 ad and ay standards [3], [4], IA (and beam search) is done in the beginning of every beacon interval. In particular, initially an AP sequentially sends sector sweep frames across its sectors, while all the clients record the signal strength of the received beams. In the next phase, each client randomly chooses a beam training slot and performs sector sweep in that slot. Several research works have proposed alternative methods that find better beams and/or reduce the beam search overhead. These works can be broadly divided into three classes: (i) exhaustive sweeping [5], [6], [7]: narrow spatial beams are used to scan all the directions exhaustively; (ii) hierarchical sweeping [8], [9], [10]: hierarchical codebooks are used to sweep all the directions; and (iii) random sweeping [11], [12], [13], [14], [15]: several random beamforming vectors are used to find the directions. A key missing piece in all these works (including the 802.11 ad/ay standard) is fairness in IA. In particular, IA provides an opportunity for all the clients to train their beams and most existing protocols rely on contention between clients as they sweep their beams. However, mmWave systems suffer from the near-far problem, in which the beams of a client that is near to the AP would have a much higher power at the AP than the beams of a competing far-client. This power imbalance can create a significant IA unfairness among competing clients, which can delay or even deny far-clients from being admitted to the network. To the best of our knowledge, this is the first paper that addresses the IA fairness problem in mmWave networks. In particular, we identify received power imbalance and poor contention protocols as the key reasons behind poor IA fairness in multi-client mmWave networks. We then propose a Joint Power control and Contention adaptation protocol ("JPOC") to address the issue. Note that IA fairness is different from throughput fairness commonly studied in networking problems [16], [17], [18]. In particular, JPOC provides an opportunity for all clients to train their beams, so that the AP has a complete information of all the clients that need resources. The amount of resources given to each client (and hence the resulting client throughput) can be then determined by the AP (see Section II), and is not addressed by JPOC. As a result, JPOC does not interfere with the desired throughput-fairness metric that the AP is aiming for.

Other works have proposed protocols to better address mmWave's mobility and blockages. Existing mmWave stan-

¹e.g., the human body alone can reduce the signal strength of a mmWave signal by more than 20 dB [1].

²We use the words "beams" and "sectors" interchangeably.

³Omni-directional transmission is susceptible to interception, which can be alleviated by the use of directional beams.

dards respond to these events by re-trigerring the sector sweep procedure and finding a new set of beams. Recent works have proposed several solutions to optimize the standard beam adaptation methods, e.g., (i) out-of-band beam search methods [19], [20] exploit the channel information from a co-existing lowfrequency radio to speed up the beam adaptation; (ii) environmental sensing solutions [21], [22] sense the reflective environment and leverage the sensed information to facilitate beam adaptation, and (iii) pro-active beam adaptation [23], [24], [25], [26] uses model-driven methods to adjust the beams before blockages happen. These solutions alleviate the impact of mobility and blockages, and ensure a smoother data communication. However, they cannot necessary find the optimal Tx-Rx beams in presence of mobility or blockages. As a result, a client may continue to contend for beam training slots in continuously recurring beam search intervals. Thus, system dynamics (e.g., mobility, blockages) can exacerbate the IA contention unfairness problem as clients frequently compete to re-train their beams. JPOC's design is complementary to all the beam adaptation related work and enhances their fairness performance in presence of system dynamics by employing PC and contention time adaptation.

B. Research Contributions

In this paper, we focus on the 802.11 ad/ay standard and design the JPOC protocol to improve the IA fairness. While we focus on WiFi, we note that the methods proposed in this paper are also applicable to the 5G cellular standard. In particular, our contributions are as follows:

- Experiments: We conduct extensive experiments with commercial-off-the-shelf (COTS) devices to identify the root cause of contention imbalance in real mmWave networks. We show that *poor contention protocols* and *power imbalance among competing beams* result in poor IA fairness among clients. The problem becomes worse in presence of system dynamics such as mobility and blockages.
- Algorithm Design: We design JPOC to address the contention unfairness during IA. JPOC's design is complementary to several existing beam search, mobility, and blockage management protocols, and can be used to enhance their fairness in presence of system dynamics. At its core, JPOC introduces a new *open-loop* and *client-side* power control mechanism and a new contention protocol that improve fairness and reduce the overhead of IA.
- Model-Driven Adaptation: JPOC adopts a model-driven approach at the AP to adapt the duration of the contention time according to the system dynamics. We show that the model can accurately predict the network traffic load and choose an optimal contention duration time for improved performance in presence of system dynamics.
- Evaluation: We extensively evaluate JPOC's performance through experiments and simulations on a comprehensive mmWave simulator. We show that compared to the standard 802.11 ad/ay protocols, JPOC substantially reduces the contention overhead and increases the IA fairness.

We elaborate on these contributions next, starting with some background on 802.11 ad/ay, followed by motivation, system design, and evaluation.

II. BACKGROUND

In this section, we describe the general type of antenna arrays that are used in mmWave radios as well as the beamforming training procedure that is used in 802.11 ad/ay.

MmWave Radios. Fig. 1(a) depicts the various components of a commercial mmWave radio. Here a Tx/Rx RF chain, which is responsible for creating a single Tx/Rx signal stream, is connected to an array of antennas. These antenna arrays are referred to as phased arrays. The phase shifter on each antenna element i shifts the phase of the signal that passes through it by multiplying the time domain RF signal by a complex coefficient ω_i . By an appropriate setting of the phase shift variables (i.e., ω_i s), we can (i) realize a beam pattern with a maximum beamforming gain (i.e., main lobe) in a particular direction, and (ii) steer the beam in the 3D space. Commercial mmWave radios also have access to an omni (or quasi-omni) antenna pattern, which is used in the 802.11 ad/ay standard.

MmWave Initial Access. Initial access in mmWave systems is a procedure that allows a client device to discover a cell, helps the AP and clients to find appropriate beams to communicate with each other, and allows the AP to send management and control information to all the clients.

In 802.11 ad/ay, this process is handled in the beginning of each beacon interval (BI) [3], [4]. The length of a BI is typically 100 ms, i.e., the BI is repeated every 100 ms. The BI is composed of two parts: (i) beacon header interval (BHI), which helps with AP discovery, beam training, and control and management information exchange, and (ii) the data transmission interval (DTI), which is used for data communication and can support different types of medium access protocols. The format of a BI is depicted in Fig. 1(d).

The BHI consists of three sub-intervals:

- Beacon Transmission Interval (BTI): The BTI comprises multiple beacon frames, each transmitted sequentially by the AP on a different sector (beam) to cover the desired directions. This process is referred to as AP sector sweep and is used for network announcement and beamforming training of the AP's sectors. During the AP sector sweep, all clients stay in reception mode using an omni (or quasi-omni) antenna pattern. Each client records the signal strength and beam ID of every sector sweep frame (SSW frame) received from the AP. Fig. 1(c) shows this operation.
- Association Beamforming Training (A-BFT): This interval is used by the client devices to train their sectors for communication with the AP. Upon completion of a successful A-BFT communication, the AP would determine and inform the clients about the beam that each client should choose for communication with the AP. To allow multiple clients to respond to an AP sector sweep, the A-BFT interval implements a contention-based response period. The A-BFT interval reserves time for multiple client

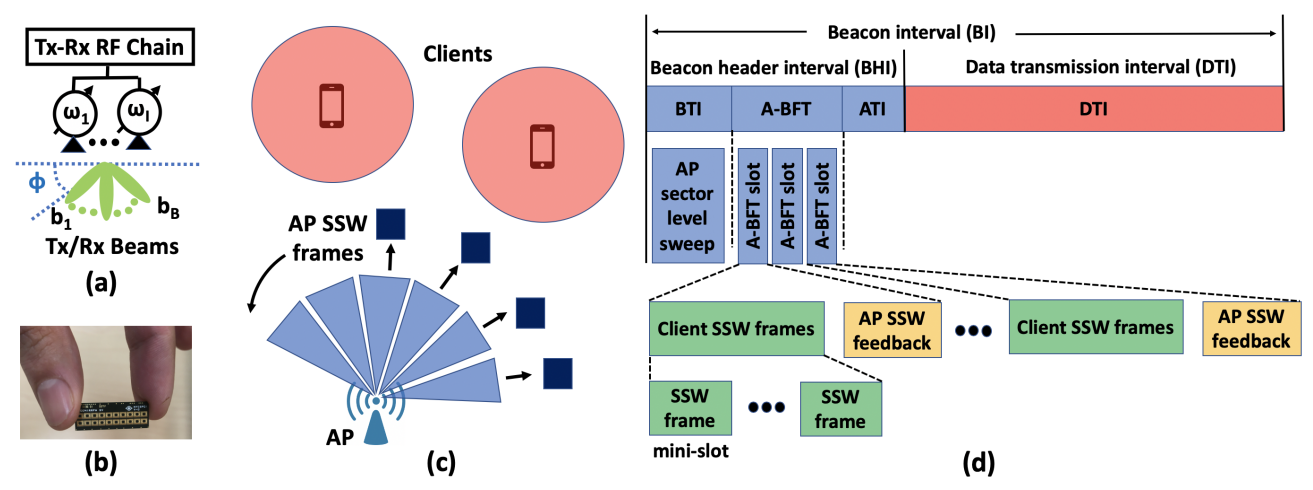


Fig. 1. (a): In a conventional mmWave radio, a single RF chain is connected to an array of antennas. There are B sectors (beams) that cover the desired 3D space; (b) A real 802.11 ad radio; (c) During the beacon transmission interval (BTI), AP sequentially sends sector sweep (SSW) frames on each of its sectors. Each client uses an omni antenna pattern and records the beam ID and signal strength of all the received SSW frames; (d): Association beamforming training (A-BFT) is composed of a few slots. A client randomly chooses an A-BFT slot to conduct its sector sweep.

sector sweeps (i.e., A-BFT slots). An overview of the A-BFT procedure is shown in Fig. 1(d). Each A-BFT slot consists of a fixed time allocation (i.e., a fixed number of mini-slots) for a number of SSW frames (transmitted by the connecting client) and one SSW feedback frame sent by the AP. Each contending client randomly selects an A-BFT slot and performs its sector sweep in that slot. Each SSW frame sent by a client contains the client information and AP beam ID that resulted in the maximum SNR at the client during the AP sector sweep (i.e., BTI). Note that during A-BFT, the AP remains in reception mode leveraging an omni antenna pattern. The AP simply records the signal strength, beam ID, and client ID for each successfully received SSW frame and then informs the client about the beam ID it should use to communicate with the AP. The contention process during A-BFT does not apply carrier sensing. Instead, a collision is detected by a missing SSW frame from the AP. Further, a client device may not be able to finish its sweep in one A-BFT slot, e.g., because the number of its sectors exceed the number of SSW frames per slot. In this scenario, a client may randomly choose another A-BFT slot in the same BHI or a later one. Finally, the 802.11 ad and ay standards only specify the maximum allowed number of A-BFT slots and leave the exact number of slots/mini-slots to vendors.

 Announcement Transmission Interval (ATI): During ATI, the AP exchanges management information with associated and beam-trained client devices. While communication during BTI and A-BFT uses the lowest modulation and coding scheme (MCS) to increase range for untrained beams, communication during ATI happens with trained beams and thus can use a higher order MCS for increased efficiency.

Medium Access Control (MAC). 802.11 ad/ay standard support three types of MAC protocols: contention based access, scheduled channel time allocation, and dynamic channel time allocation. The latter two mechanisms uses time division multiple access (TDMA) and polling (similar to 802.11 PCF) to share resources among the clients.

III. MOTIVATION

In this section, we present experimental results to motivate the existence and prevalence of the contention unfairness problem in mmWave networks with commercial-off-the-shelf (COTS) 802.11 ad devices. We first conduct experiments to characterize the variations in SNR as a function of beam ID and client location. We show that there is a significant imbalance in the received power of clients' beams as a function of client location, which can cause severe contention unfariness during the A-BFT interval. Next, we show how network dynamics such as mobility and blockages can retrigger client participation in the A-BFT contention.

Experiment Setup. We setup a single-cell mmWave network in an indoor office environment using a few Talon AD-7200 routers and an Acer TravelMate laptop. We use one router as an AP, one router as a packet sniffer, and one router configured as a client device. We use the TravelMate laptop as a different client device. Fig. 2(a) shows a picture of our equipment. All of our devices use Qualcomm's QCA9500 802.11 ad chip, which uses a 32-antenna phased array with a single Tx-Rx RF chain. The default firmware for the AD-7200 router neither supports A-BFT SNR dump nor sniffer mode. To enable these features, we modified the default firmware using Nexmon framework [27] and installed that on the sniffer router to gather low-level signal statistics. This framework is a jailbreak into the 802.11 ad default firmware, which allows to amend patches in C language rather than assembly and it also provides new attributes and programs such as a GCC plugin. Talon AD-7200 routers with Nexmon firmware can be configured as either an AP, client or sniffer [26], [27]. We place the sniffer router next to the AP. In all of our experiments, we let the clients get connected to the AP but measure their packets' signal strengths at the sniffer. This is because, as mentioned, the default AP firmware (which should be used for client connectivity) does not provide signal statistics.

Sample Beam SNR values for two Different Client Locations. We first conduct an experiment to see how distance

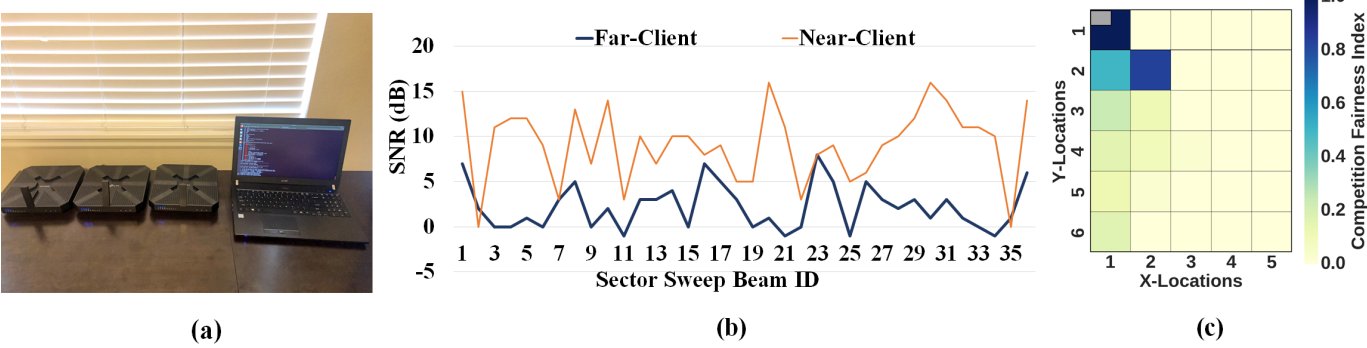


Fig. 2. (a): We conduct experiments leveraging three Talon AD-7200 routers and an Acer TravelMate laptop; (b): SNR of near- and far- clients' beams versus sector ID; (c): Fairness heatmap. Near-client location is fixed. The other client is placed in different cells to derive the fairness value. The gray box at the top left corner shows the AP location. Without power control, the competition fairness index at many locations is close to zero.

between clients and AP affects the SNR of the clients' beams at the AP, and hence their contention during the A-BFT interval. We place one client in front of the AP at 1 m distance ((x,y) location (1,1) in Fig. 2(c)). We refer to this client as the near-client. We let the client conduct its sector sweep and get associated to the AP. The orange graph in Fig. 2(b) shows the SNR of the near-client's beams as a function of its beam IDs. We observe that all beams achieve a minimum SNR of 0 dB with a few beams achieving SNR values as high as 16 dB. We next use a second client and place it at 5 m distance from the AP ((x,y) location (3,3) in Fig. 2(c)). We let the client get associated to the AP and plot the resulting beams' SNR values on the same figure. We refer to this client as far-client. We observe that almost all of the far-client beams achieve a lower SNR than the near-client beams. As a results, whenever the two clients choose the same A-BFT slot to conduct their sector sweeps, most of the near-client's SSW frames would be captured⁴ by the AP, whereas the far-client would not be heard or acknowledged. The far-client can only get associated to the AP if it chooses a different A-BFT slot in the same or next beacon interval.

Prevalence of Contention Imbalance. Our next goal is to characterize the prevalence of contention unfairness caused by received beam power imbalance across different locations in a typical indoor environment. Fig. 2(c) shows the layout of our experiment setup and the corresponding fairness heatmap. Our AP is located at the top left corner (gray box in Fig. 2(c)). We place the near-client in (x,y) location (1,1) and let it associate to the AP. We next record the SNR values of its beams at the AP. We next place the second client in every other (x,y) location, allow it to associate to the AP, and record the SNR values of its beams at the AP. Finally, we take the following steps to characterize the competition fairness among the two clients from all of our recorded data. Let SNR_i^{near} denote the near-client SNR value (in dB) for beam index i, and $SNR_i^{other(j)}$ show the SNR value of the other client at

location j as it uses beam index i. Let $S^{other(j)}$ (success rate of the other client at location j be defined as the total number of beams (is) for which $SNR_i^{other(j)}-SNR_i^{near}$ is ≥ 3 dB. Assuming that the two clients send their SSW frames in the same A-BFT slot, these are the beams that can be decoded at the AP due to the capture effect. Similarly, we define S^{near} (success rate of the near client) as the total number of beams for which $SNR_i^{near}-SNR_i^{other(j)}$ is \geq 3 dB. We then define the competition fairness index at other client location j as $\frac{S^{other(j)}}{S^{near}}$. Fig. 2(c) shows the heatmap of this index. We observe that sector SNR imbalance is quite prevalent in typical indoor environments. Only when the other client is located in the same (x,y) cell as the near-client the fairness index is close to 1. As its moves to other locations, all of its beams' SNR values quickly drop to below the SNR values of the nearclient's beams. In other words, it will lose contention in a majority of other locations, if both clients choose the same A-BFT slot to conduct their sector sweeps.

Frequency of Client Participation in A-BFT. The degree of throughput unfairness depends on the frequency of clients' participation in A-BFT, which itself depends on systems dynamics and parameters. For example, assume only a single A-BFT slot, one near-client and one far-client. If the nearclient participates in A-BFT in each beacon interval, then the far-client would continuously lose the contention and would achieve a zero throughput. We have conducted several experiments to characterize what can re-trigger client participation in A-BFT. We have omitted the experimental results due to the page limitations, but provide a summary here: (i) Mobility: when a client moves, the initially selected sectors would not be optimal any longer. Hence, the client may participate in the next A-BFT to re-train its beams; (ii) Blockages: when blockage happens, the client would completely lose the connection to the AP. In an uplink scenario (e.g., uplink UDP), the client would wait until the next beacon interval to receive the AP SSW frames and then would participate in A-BFT to find an alternative path to the AP; and (iii) Association to a **New AP:** when a client moves, it can discover a new AP with a better channel quality. The client would then participate in A-BFT to find beams to the new AP.

 $^{^4}$ When two frames arrive at the same time at the AP, the frame with an x dB or more signal strength can be correctly decoded, whereas the other frame would be lost. The exact value of x depends on the frames' MCS values, e.g., 3 dB with the lowest MCS, which is used in SSW frames. This phenomenon is referred to as the "capture" effect [28].

IV. DESIGN OF JPOC

We now present our joint power control and contention slot adaptation protocol (JPOC) that addresses the identified challenges. At a high level, JPOC incorporates three innovations to achieve fairness in mmWave initial access. First, it introduces an uplink power control mechanism that is executed by each client device. This makes sure that for each client, only a few of its beams achieve high enough SNR at the AP so that they can be correctly decoded, whereas the rest of the client beams cause little to no interference at the AP. Second, we suggest a new A-BFT protocol and a mechanism for the AP to predict the optimal number of contention mini-slots (as a function of number of competing clients). This both reduces the overhead of initial access as well as the time it takes for clients to establish connection with the AP. Third, the AP continuously adapts its parameters in order to handle any system dynamics.

A. Power Control Design

The goal of our power control algorithm is to allow each client choose a transmission power such that only a few of its beams can be received at the AP. These are the client beams that without power control would have achieved the highest SNR values at the AP. We refer to these clients beams as goodbeams. Now, assume that such a power control mechanism is executed by each client. As a result, when a near and a far client simultaneously perform their sector sweeps, the far client would not be drawn in the interference caused by the near client (Fig. 3 shows this operation). This increases the initial access fairness among competing clients and both clients would be able to establish a connection with the AP with a much lower number of required mini-slots. Note that the power control mechanism is used only during the A-BFT interval and would be disabled during data transmission for fast data communication between the AP and client.

In this section, we discuss how a client can choose an appropriate transmission power. Note that when PC is employed, the client uses the **same** transmission power for all of its SSW frames as it performs sector sweep during A-BFT. We assume that without PC, each client uses the maximum transmission power (which is what is implemented in our COTS devices). Thus, when PC is employed, the selected transmission power is either reduced or unchanged.

We take the following approach. For every client, our goal is to select the client transmit power such that its *best beam* achieves a desired signal strength (and hence SNR) at the AP. Note that the *beam best* is not known prior to sector sweep.

Let RxP_{max}^{AP} denote the desired signal strength at the AP. We use the RxP_{max}^{AP} notation, as for each client, its best beam would achieve this value. Further, as PC is employed many of the client beams would cause little to no interference at the AP (Fig. 3). Also, note that RxP_{max}^{AP} is the same across all the clients. Now, a desired maximum received power at the AP is equivalent to aiming for a desired maximum SNR at the AP, as the two values are related to each other as follows

$$\gamma(dB) = Rx P_{\max}^{AP}(dBm) - NoisePower^{AP}(dBm) \quad \ (1)$$

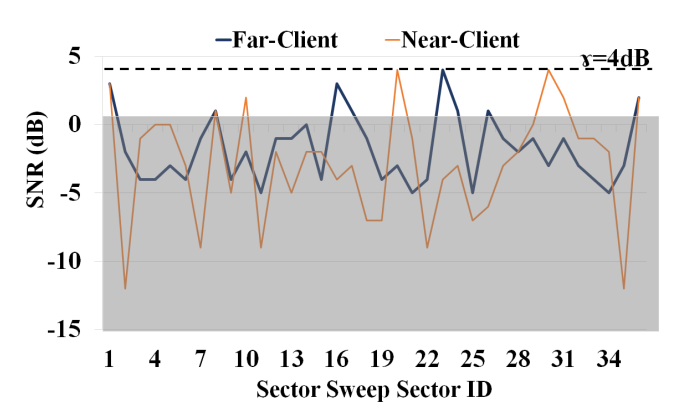


Fig. 3. SNR of near- and far- clients' sectors when power control (PC) is employed. These are the same two clients that without PC received the SNR values depicted in Fig. 2(b). Each client adjusts its transmit power such that its best beam achieves an SNR equal to γ at the AP. Beams with less than 1 dB SNR cannot be decoded at the AP and cause zero to no interference. Clients' beams that fall into the shaded gray box depict such beams. In this example, $\gamma=4$ dB.

Here, γ denotes the desired SNR and $NoisePower^{AP}$ denotes the AP noise power. Noise power is a function of channel bandwidth and AP noise figure, which are all known parameters at the AP. Now, for a sector sweep frame to be decodable at the AP, its SNR should be at least equal to 1 dB. Thus, we choose a γ higher than 1 so that for each client potentially a few beams achieve high enough SNR at the AP as opposed to just one (e.g., in Fig. 3 we set γ equal to 4).

Therefore, for a desired γ , all the client has to do is to *select* a transmit power such that

$$RxP_{\max}^{AP}(dBm) = \gamma(dB) + NoisePower^{AP}(dBm)$$
 (2)

To help clients with their PC, we let the AP announce the value of $RxP_{\rm max}^{AP}$ by using Eq. (2) and choosing a desired γ . The calculated value is included in the SSW frames transmitted by the AP during the BTI interval.

We next proceed to discuss how each client can choose its transmit power such that its maximum received power at the AP (as the client performs sector sweep) is equal to $RxP_{\rm max}^{AP}$. Consider a client (CLT) and let i denote the client beam index that achieves the maximum received power at the AP. Then, from the path loss formula we have

$$RxP_{\max}^{AP} = P_T^{CLT} + G_T^{CLT}(i) + G_R^{AP} - PL$$
 (3)

Here, P_T^{CLT} is the client transmission power, $G_T^{CLT}(i)$ is the client beamforming gain as it uses beam index i, G_R^{AP} is the AP's beamforming gain (note that during the client sector sweep, the AP uses a fixed omni beam for reception), and PL is the path loss component between the AP and client⁵.

Next, consider the preceding AP sector sweep (i.e., BTI) and let j denote the AP beam index that achieved the highest SNR at the client. Then

$$RxP_{\max}^{CLT} = P_T^{AP} + G_T^{AP}(j) + G_R^{CLT} - PL$$
 (4)

⁵In LTE, clients explicitly estimate the PL with the help from eNB, and use that for uplink PC [29], [30]. We do not explicitly calculate PL.

Note that RxP_{\max}^{CLT} (i.e, the maximum received power at the client device as the AP performs sector sweep) is a known value at the client. By subtracting Eq. (4) from Eq. (3), removing the common PL term, and rearranging the parameters we have

$$\begin{split} P_{T}^{CLT} &= RxP_{\max}^{AP} - RxP_{\max}^{CLT} + \\ (G_{R}^{CLT} - G_{T}^{CLT}(i)) + (G_{T}^{AP}(j) + P_{T}^{AP} - G_{R}^{AP}) \end{split} \tag{5}$$

Now, $(G_T^{CLT}(i)-G_R^{CLT})$ can be approximated as the array gain (or maximum beamforming gain) of the client antenna array⁶, which is a known variable at the client device. Similarly, $(G_T^{AP}(j)-G_R^{AP})$ is the maximum array/beamforming gain of the AP's antenna array, which is known at the AP⁷. In JPOC, the AP calculates the value of $(G_T^{AP}(j)+P_T^{AP}-G_R^{AP})$ and adds this information to the message that is sent on each of its SSW frames during the AP sector sweep (i.e, BTI).

As a result, each client would have all the necessary information to use Eq. (5) and find the optimal transmission power (P_T^{CLT}) that it should use for its sector sweep. Note that if the calculated P_T^{CLT} is higher than the maximum possible Tx power, the client simply uses the maximum Tx power.

B. A New A-BFT Design and Optimal Mini-Slot Number Determination

As discussed in Section II, the 802.11 ad and ay standards divide the A-BFT time into slots and mini-slots, which as we show later in Section V-C can unnecessarily increase the A-BFT overhead. We propose to only use mini-slots. In particular, in JPOC, the AP determines the number of mini-slots that would be dedicated to A-BFT interval and announces that during its sector sweep (i.e., BTI interval). Let M denote the number of mini-slots and B the number of client beams. Then, during A-BFT, each client randomly selects B out of these M mini-slots and transmits on a different beam during each mini-slot. Fig. 4 shows this operation.

The only remaining task in JPOC's A-BFT design is to answer how should the AP determine the optimal number of mini-slots? We conduct theoretical analysis to answer this question. Let K denote the number of good-beams (i.e., the number of client beams with decodable SNR at the AP) and N the number of clients that are contending during A-BFT. We assume that K is the same across all clients⁸. We also assume that non good-beams do not collide with good-beams at the AP⁹, i.e., only a good-beam transmission can be successful,

 $^6\mathrm{The}$ approximation is because a selected beam does not maintain the beamforming gain in its entire beamwidth. In fact, the beamforming gain drops by 3 dB towards the edges of the selected beam. Thus, in all of our evaluations in Section V, we remove 3 dB from the calculated $(G_T^{CLT}(i)-G_R^{CLT})$ and $(G_T^{AP}(j)-G_R^{AP})$ values. This slightly reduces JPOC's performance but ensures that the best beam achieves γ or a slightly higher SNR at the AP.

 7 All of our COTS radios use a fixed number of pre-determined beams for IA, which makes it easy to use Eq. (5) and find the Tx power. If dynamic beamforming is employed (i.e., the selected IA beams are continuously changed), then we need to employ a model to determine the variations in beamforming gains (e.g., $(G_T^{CLT}(i) - G_R^{CLT}))$) before using Eq. (5).

⁸This is because with PC, the similarity in the number of good-beams across all clients increases. We will show this through experiments in Section V-A.

⁹This is because non good-beams cause very little interference at the AP. For example, see the gray box in Fig. 3, which contains the non good-beams.

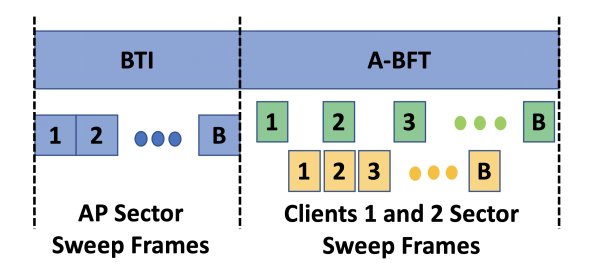


Fig. 4. There are M mini-slots in the A-BFT interval. Each client randomly chooses B mini-slots and sends its SSW frames in them. The AP can acknowledge all clients during the ATI or as part of the A-BFT.

and only if no other client transmits with a good-beam in the same mini-slot. Then, for a given client, the transmission probability in a mini-slot (p) is $\frac{K}{M}$ (we ignore non good-beam transmissions, as they would not be detected at the AP).

Now, consider a client that is currently transmitting with a good-beam. The probability of this good-beam transmission to be successful is equal to $(1-p)^{N-1}$.

Let P_0 denote the **targeted** failure probability for a client, i.e., the desired probability that a client that participates in A-BFT cannot establish a connection with the AP. P_0 is a design parameter used in JPOC. Our goal is to select a number of mini-slots (M) such that the probability of a client not being able to establish connection to the AP during A-BFT (i.e., P[failure]) is less than P_0 . Thus, we have

$$P[failure] = (1 - (1 - p)^{N-1})^K \le P_0 \tag{6}$$

Replacing p with $\frac{K}{M}$ in Eq. (6) and after a series of simplifications we have

$$M_{opt} = \lceil \frac{K}{1 - (1 - P_0^{\frac{1}{K}})^{\frac{1}{N-1}}} \rceil$$
 (7)

Thus, with known K and N, the optimal M is the smallest integer that satisfies Eq. (7) ($\lceil \rceil$ shows the ceiling operator). In section V, we conduct extensive experiments that show the statistics (e.g., average) number of good-beams with COTS devices. We use these statistics to choose K.

The only unknown parameter in determination of M_{opt} in Eq. (7) is the number of clients that will participate in A-BFT contention (i.e., N). We next propose a method so that the AP can estimate N. At a high level, JPOC uses statistics from contention in the previous A-BFT rounds to determine the number of competing clients in those rounds, and then uses those estimates to determine the number of clients that would compete in the current A-BFT round.

Consider a **previously** completed A-BFT round, e.g., round t', which used a given number of mini-slots $(M^{t'})$. Upon completion of A-BFT in that round, the AP counts the number of A-BFT mini-slots in which the received energy was below the detectable SNR threshold. An empty A-BFT mini-slot means that either no client attempted to transmit in that mini-slot or the selected beam did not produce enough energy at

the AP. Thus, we have

$$\frac{\# \ of \ empty \ mini - slots}{M^{t'}} \approx (1 - p)^{N^{t'}} = (1 - \frac{K}{M^{t'}})^{N^{t'}}$$

$$\implies \boxed{N_{\text{est}}^{t'} \approx \frac{\log(\frac{\# \ of \ empty \ mini - slots}{M^{t'}})}{\log(1 - \frac{K}{M^{t'}})}}$$
(8)

Here, $N_{est}^{t'}$ is the AP estimate of the number of clients that competed in A-BFT round t'. Next, we find an average of $N_{est}^{t'}$ over the previous T rounds to compute the expected number of competing clients in the current A-BFT round t, as follows:

$$N_{expected}^{t} = \frac{N_{est}^{t-1} + N_{est}^{t-2} + \dots + N_{est}^{t-T}}{T}$$
(9)

The averaging over the past T rounds is to dampen any oscillations. In our simulations, we observed a smooth performance with rapid adaptation to system dynamics with T=5. Thus, we set T to $\min(t,5)$ to also account for initialization.

JPOC's Mini-Slot Adaptation Algorithm: A JPOC AP continuously adapts the number of mini-slots (M) according to the system dynamics. It takes the following steps to determine the optimal number of mini-slots in the current A-BFT round t: For a given number of good-beams (K) and desired client failure probability (P_0) , it first uses Eq. (8) to determine the number of clients that participated in the previous T rounds of A-BFT contention. It then uses Eq. (9) to estimate the expected number of competing clients in round t and plugs that value into Eq. (7) to determine the optimal number of mini-slots that should be used in the current A-BFT round t. The selected value of t is then announced to all clients during the AP sector sweep (i.e., BTI). For the initial value of t (e.g., when an AP is initially turned on), we use a default value of 64 mini-slots. We also set the minimum value of t to 36.

C. Protocol Overhead

JPOC introduces three types of overhead that are added to each SSW frame transmitted by the AP during its sector sweep: (i) the desired maximum received power at the AP (RxP_{max}^{AP} from Eq. (2)), which even for $\gamma=4$ and AP noise power of -90 dBm would at most need 8 extra signaling bits, (ii) ($G_T^{AP}(j)+P_T^{AP}-G_R^{AP}$), which assuming a 32-antenna array and 20 dBm transmission power would at most need 6 extra bits, and (iii) the number of mini-slots (M), which would be an extra 6 bits for up to 128 mini-slots. This minor increase in control bits substantially improves the system fairness and reduces the overall overhead as we show next¹⁰.

V. PERFORMANCE EVALUATION

In this section, we evaluate the performance of JPOC through both experiments and simulations. We first use our experimental setup from Section III to evaluate the power control aspect of JPOC with COTS devices. However, even the jailbreak framework does not allow

 $^{10}{\rm Eq.}$ (5) only needs the value of $(RxP_{max}^{AP}+G_T^{AP}(j)+P_T^{AP}-G_R^{AP})$ to find P_T^{CLT} . Thus, we can combine (i) and (ii) to further reduce the signaling.

us to change the A-BFT aspect of 802.11 ad. Thus, we next use simulations with a simplified channel model to characterize the accuracy of JPOC in determining the number of competing clients and adjusting the number of mini-slots, accordingly. Next, we use a comprehensive simulator with a standard compatible channel model and in the presence of system dynamics to characterize the full range of system performance in terms of fairness and protocol overhead.

A. Impact of Power Control (PC)

Experimental Setup. We use the same equipment and experimental setup of Section III. In particular, we modified the default firmware on the sniffer router using the Nexmon framework. We then obtained the corresponding SNR dumps and used them to derive the results of this section.

Impact of PC on the Number of Good-Beams. We first study how client-side PC impacts its number of beams with detectable SNR at the AP (i.e., the number of the client's good-beams). We consider the indoor setup of Fig. 2(c), which provides a rich variety of channel conditions, and take multiple samples in each grid-cell with different client orientations. For a given client location and orientation, we obtain the SNR dump of all the client's beams for three different power control (PC) mechanisms: (i) without (W/O) PC: each clients uses the same maximum transmission power; (ii) with (W) PC and $\gamma = 10$, and (iii) with PC and $\gamma = 4$. Recall from Section IV-A that γ denotes the desirable SNR at the AP, i.e., each client adjusts its transmission power such that the resulting SNR of the best beam at the AP is equal to γ . Fig. 5(a) shows the distribution of good-beams across all experiments. We divide the number of good-beams (x-axis) into six brackets (from [1] to 6] to [31 to 36]), and plot the percentage of clients whose number of good-beams falls into each bracket. We observe that without PC (i.e., the default 802.11 ad implementation), clients are almost equally distributed across all the brackets. Further, clients could have as high as 31-36 or as low as 1-6 goodbeams. When PC is employed, the number of good-beams would depend on the selected γ . As γ is reduced, the number of good-beams reduces, and the similarity in the number of good-beams across clients increases. For example, when γ is 10, most clients would have 1 to 24 good-beams, and close to 45% of clients would have 7-18 good-beams. Further, no client would have 31 or more good-beams. As γ is further reduced to 4, more than 90% of clients would have 1-12 good-beams, and no client would have 18 or more good-beams (in fact, our dataset shows that no client would have more than 14 good-beams). Our results show that PC has the potential to increase the contention fairness among clients. The similarity in the number of good-beams increases across clients as PC is employed. Further, these beams would have a much closer range of SNR values at the AP.

Impact of PC on Fairness. We next study the effect of PC in alleviating unfairness among competing clients. We consider the indoor environment discussed in Fig. 2(c). Further, we consider the same extreme scenario: a near-client in (x,y) cell location (1,1) and the location of the *other* client in

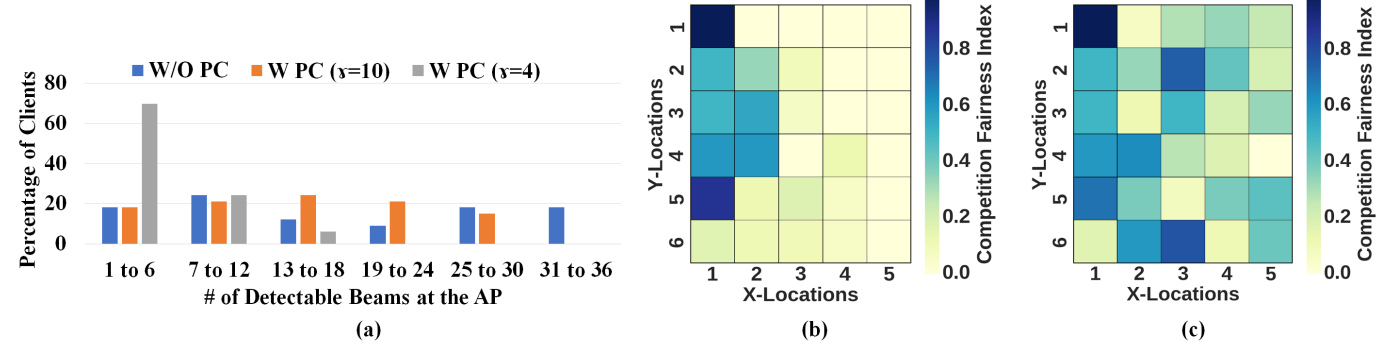


Fig. 5. (a): Distribution of the number of good-beams with (W) and without (W/O) PC. With PC and $\gamma = 4$, close to 70% of clients would have 1-6 good-beams; (b) and (c): Competition fairness index for γ equal to 10 and 4, respectively. PC drastically improves fairness, particularly with a smaller γ . Note that even with PC, there are client locations that still cannot compete fairly in presence of the near-client. JPOC improves the performance of such clients through an appropriate selection of the number of mini-slots, so that these clients can also send their SSW frames.

every other cell. We leverage the PC mechanism at all the locations and use two different γ values: 10 and 4. Next, we use the same setup of Fig. 2(c) to obtain the clients' beams SNR values and then derive the competition fairness index $(\frac{S^{other(j)}}{S^{near}})$ between the near-client and the *other* client at every other location j. Recall from Section III that S^{near} (i.e., nearclient's success rate) is the fraction of near-client's beams with 3 dB or more SNR than the other client's beams. Fig. 5(b) and (c) depict the corresponding fairness index values for γ equal to 10 and 4, respectively. Note that we are considering a very extreme scenario, with the near client in a line-of-sight channel condition and very close to the AP. As a result, a majority of the near-client's beams have a high SNR. However, our results show that compared to the fairness heatmap of Fig. 2(c) that did not use PC, leveraging PC substantially improves the fairness. This is because with PC, different clients would have a more similar number of good-beams, and with closer SNR values at the AP. The fairness further improves for a smaller γ , which is due an even more similarity between the number of good-beams, as we showed in Fig. 5(a).

B. Modeling Accuracy and Performance

Our jailbreak framework allows us to re-configure some hardware parameters and gather signal statistics, however, we still cannot change the A-BFT design. Thus, we resort to simulations to evaluate JPOC's performance. In this section, we use a simulator with a simplified channel model to evaluate JPOC's accuracy in determining the failure rate and the number of competing clients.

Simulation Setup. We simulated a single cell with one AP and a varying number of competing clients (N) and goodbeams (K). Each client has access to K good-beams. We ignore the non good-beams at the clients as these beams would not produce enough energy at the AP. For a given number of mini-slots (M), each client randomly selects K out of M to transmit on its good-beams. A client can establish a link with the AP if at least one of its good-beam transmissions is successful. This happens if no other client transmits at the

same time with a good-beam. Unless otherwise specified, each simulation data point is a result of 100 realizations.

Failure Rate Prediction. In Section IV-B (Eq. (6)), we presented a model to calculate the probability that a client would fail in establishing a connection with the AP (P[failure])in a single A-BFT interval. We then used this model to determine the optimal number of mini-slots for a targeted failure rate (P_0) . In this section, we evaluate the accuracy of this model. For a given number of mini-slots (M), number of competing clients (N), and number of good-beams (K), we first conduct simulations to determine the actual failure rate for each client. We next find the average failure rate across all the 100 simulation realizations. The blue graphs in Fig. 6(a) represent the average of these actual failure rates as a function of number of clients (N) and for two different values of M(32 and 64), assuming 4 good-beams at each client. We then use Eq. (6) to find the failure probability predicted by our model, and use red stars (* and x) to show them on the same figure. We observe that irrespective of the number of clients, mini-slots, and good-beams, our model presented in Eq. (6) estimates the failure rate with a very high accuracy¹¹. Note that the results also mean that for a targeted failure rate, and for a known number of clients and good-beams, our model can accurately predict the optimal number of mini-slots.

Accuracy in Determination of the Number of Clients (N). In Section IV-B (Eq. (8)), we presented a model that the AP can use to estimate the number of clients that participated in a given A-BFT round. The AP can then use the estimate to determine the number of mini-slots that should be used in a future A-BFT round. In this section, we verify the accuracy of our model to estimate the number of clients in an A-BFT round. For a single simulation realization, we fix the number of clients, set the number of good-beams (K) to 4, and the number of mini-slots (M) to 60. Next, each client randomly selects K out of M mini-slots and transmits in them. Note that the number of competing clients (N) is not known at

¹¹We conducted additional simulations to verify our model accuracy with a varying number of good-beams. We observed a similar accuracy.

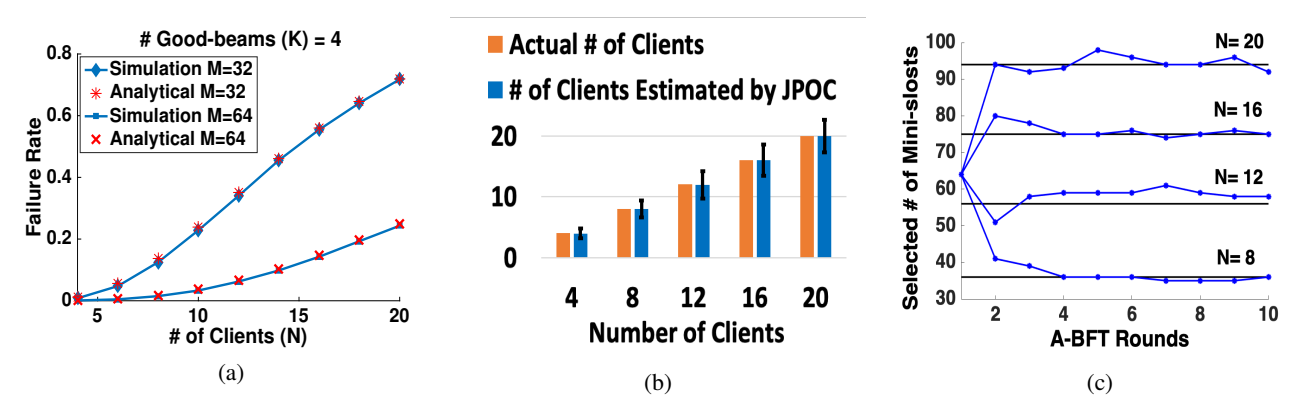


Fig. 6. (a): Simulated failure rate vs its value predicted by our model; (b): Number of actual competing clients vs the value estimated by our model. JPOC accurately estimates the number of competing clients, however, there is a non-zero standard deviation; (c): Evolution of mini-slot size (M) as a function of A-BFT round for four different and fixed client numbers. M_{opt} for each given number of clients is plotted as a straight black line.

the AP. The AP counts the number of empty mini-slots (i.e., mini-slots with zero good-beam transmissions) and then uses Eq. (8) to estimate N. For every given number of clients, we do 100 simulation realizations, and derive the mean and standard deviation of these estimated N values. Fig. 6(b) shows the corresponding results as a function of the number of clients. Here the orange bars represent the actual number of clients and the blue bars represent the values estimated by our model. We observe that irrespective of the actual number of clients, on average we can accurately predict it. However, there is a non-negligible standard deviation in our model prediction. This is because between different simulation realizations, there could be a notable variation in the number of measured "empty mini-slots" as observed by the AP, which creates a variation in the estimated number of clients. We have conducted additional simulations with different number of good-beams, which showed a similar performance.

Temporal Evolution of the Number of Mini-Slots. We next study how JPOC adapts the number of mini-slots (M) at the AP as a function of time (i.e., A-BFT round). In particular, we consider the mini-slot adaptation algorithm discussed in Section IV-B, and plot how JPOC adapts the mini-slot size for a fixed number of competing clients. Note that as the number of clients is fixed, there is a single and optimal value of Mthat can be found from Eq. (7). However, JPOC does not have an accurate estimate of N to derive M, and uses the estimation methods discussed in Eqs (8) and (9) to estimate N and choose M. Fig. 6(c) depicts JPOC's adaptation of Mfor four different and fixed values of client numbers. Recall from JPOC's algorithm in Section IV-B, that we set the initial value of M to 64. The x-axis in the figure denotes the A-BFT round. For each graph, we also derive the optimal value of M (leveraging Eq. (7) and setting P_0 to 0.1) and plot it as a straight black line. Our results show that JPOC quickly gets very close to the optimal value of M (in most cases in just one round), with dampened oscillations in future rounds (due to the averaging in the estimation of the expected number of clients as we did in Eq. (9)). Note that as explained in the previous paragraph, there will always be some minor oscillations around the optimal M. This is because the accurate number of competing clients is not available at the AP.

System Performance as a Function of Churn Rate. We next study how sudden variations in the number of clients that compete in an A-BFT round (i.e., churn rate) affect JPOC's performance. We fix the number of clients (N) to 20, the desired failure rate (P_0) to 0.1, and the number of good-beams (K) to 4. We let JPOC run for 2 A-BFT rounds and adjust the number of mini-slots (M) so that the failure rate is close to P_0 . Next, we simulate four scenarios in which the number of competing clients in the third A-BFT round suddenly increases to 22, 24, 30, and 40 (i.e., churn rates of 10, 20, 50, and 100 percent). We observed that the resulting client failure rate in the third A-BFT round increases to 0.13, 0.16, 0.26, and 0.44, respectively. Note that the sudden increase in the number of competing clients reduces the number of empty mini-slots and as a result JPOC would choose a higher number of minislots (M) in the fourth A-BFT round (similar to the results of Fig. 6(c)). This, reduces the average failure rate to 0.11 in the fourth A-BFT round. JPOC easily tolerates moderate churn. In a high churn scenario, JPOC quickly reduces the failure rate within two beacon intervals. The most extreme scenario happens if the number of clients drastically changes every beacon interval. One way to combat such extreme scenarios is to reduce the beacon interval, e.g., set the default value to 50 msec instead of 100 msec for faster adaptation to churn.

C. Comparison Against 802.11 ad/ay

Simulation Setup. We use a comprehensive mmWave simulator to evaluate JPOC's performance with standard-compatible channel models. We consider an indoor deployment with clients randomly and uniformly deployed in a 25 m radius cell and the AP deployed at the center of the cell. We create channels between every client and the AP according to the standardized channel model [31]. We set the center frequency to 60 GHz, and noise figure to 7 dB. All of our devices use the same channel for communication with 2 GHz of bandwidth. Each device has access to a 32-antenna (8x4) phased array with a single Tx-Rx RF chain, and uses 36 beams to cover 120° of Azimuth and 120° of elevation. We consider uplink traffic and assume that clients are fully backlogged with

UDP traffic. We set the duration of a beacon interval to 100 msec and run each simulation realization for 10 seconds. We use a probabilistic model to create mmWave blockages [31]. When blockage happens, a client's data transmission gets lost and the client needs to compete in the next A-BFT round to obtain a new path to the AP. The blockage occurrence probability is a function of blocker density (e.g., number of humans) and is a variable in our simulator. Finally, we use a time-fair TDMA MAC scheduler at the AP. The scheduler equally divides the data transmission time interval between all of the associated clients and informs the clients about their schedules at the beginning of every ATI interval.

802.11 ad/ay Implementation. In addition to JPOC, we implement 802.11 in our simulator. Our implementation of 802.11's A-BFT design is according to the standard protocol (see Section II). Specifically, it does not perform any uplink PC. Moreover, its A-BFT interval is composed of a few slots. Each slot is itself composed of a few mini-slots. The standard does not specify how a device should adapt the number of slots/mini-slots according to the traffic load. It only specifies the maximum allowed number of slots (e.g., 8 in ad [3]), and leaves the specific implementation to the chip manufacturer. For example, our 802.11 ad router does not change the number of slots according to the network traffic.

Fairness Definition. We compare the Jain's fairness index across the different schemes. Let x_c denote the total time allocated to client c in a simulation realization. Then, Jain's fairness index is defined as $(\sum_{c=1}^N x_c)^2/(N\sum_{c=1}^N x_c^2)$. When the fairness value is closer to 1, it means that the distribution of air-time among clients is equal, whereas when the fairness index is less than one, it means that the air-time distribution among clients is imbalanced. Note that as we discussed in our simulation setup, our AP uses a static TDMA schedule during the data transmission interval and divides the time equally among its associated clients. Thus, with a fair competition we expect the Jain's fairness index to be close to 1.

Fairness Comparison. Fig. 7(a) shows the Jain's fairness index values across two schemes: (i) 802.11 ad/ay, and (ii) JPOC. In our implementation of 802.11, we set the number of slots to 8, and the number of mini-slots to 36. Thus, a single client can fully perform its sector sweep in a single slot. The simulation corresponds to 16 clients and shows the fairness index as a function of blockage occurrence probability. We observe that JPOC maintains a high fairness among the clients irrespective of the blockage probability, whereas 802.11's performance drastically drops with a higher blockage probability. This is because JPOC (i) uses a PC mechanism that reduces the disparity in the number of good-beams across all clients, and (ii) adapts the number of mini-slots (M) according to its estimate of the number of competing clients.

Protocol Overhead. It is possible to improve 802.11's performance by using a higher number of slots. In this section, we examine the minimum required number of slots (and minislots) to achieve a desired client failure rate. Note that the 802.11 ad/ay standard do not specify how an AP should adapt its number of slots/mini-slots according to the traffic load. We

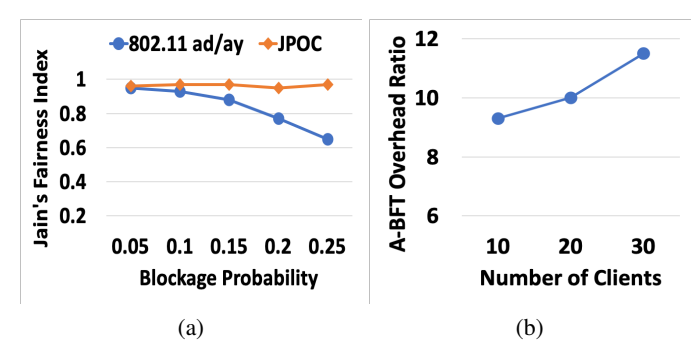


Fig. 7. (a): Fairness comparison between JPOC and 802.11 ad/ay; (b): Overhead of 802.11 to JPOC with 10% targeted failure rate.

set the targeted client failure rate to 10%, and assume a 20% blockage occurrence probability. Next, we conduct simulations to find the minimum number of 802.11 slots that meet the failure rate. Each of our 802.11 slots is composed of 36 minislots to accommodate all client sector sweep frames. Fig. 7(b) shows the ratio of the number of 802.11 A-BFT mini-slots to JPOC as a function of the number of clients. We observe that the required number of mini-slots increases by more than 9x.

VI. CONCLUSION AND FUTURE WORK

We studied the problem of initial access fairness in 802.11ad/ay networks. We showed that as clients train their beams, there exists a severe power imbalance between different clients' beams at the AP. We showed that this power imbalance coupled with poor 802.11 ad/ay contention protocol design, substantially reduces the IA fairness among competing clients. We then proposed a joint power control and contention adaptation protocol (JPOC) to address this unfairness problem. We characterized the average performance of JPOC through simulations with uniformly distributed clients. We showed that compared to 802.11 ad/ay, JPOC substantially reduces the contention overhead and increases the system fairness.

For our future work, we intend to characterize the full range of fairness-overhead tradeoffs that may not be captured through a uniform client distribution. For example, we have observed rare practical scenarios in which a near-client has many good-beams and all with similar SNR values at the AP. This diminishes the gains of PC and causes wide variation in the number of good-beams across all clients, which limits the accuracy of our model to determine the number of mini-slots. In such cases, JPOC may not achieve perfect fairness.

VII. ACKNOWLEDGEMENTS

We would like to thank our shepherd, Kate Lin, and the anonymous reviewers for their valuable feedback, which helped in improving the presentation of the paper. This research was supported in part by an NSF CAREER award (CNS-1942305). We would like to thank the 2018 NeTS CAREER panelists for their valuable feedback on our proposed project, and the 2019 panelists for funding our research.

REFERENCES

- [1] C. Gustafson and F. Tufvesson, "Characterization of 60 GHz shadowing by human bodies and simple phantoms," in *Proceedings of European* Conference on Antennas and Propagation, 2012.
- [2] M. Gapeyenko, A. Samuylov, M. Gerasimenko, D. Moltchanov, S. Singh, M. R. Akdeniz, E. Aryafar, S. Andreev, N. Himayat, and Y. Koucheryavy, "Spatially-consistent human body blockage modeling: a state generation procedure," in *IEEE Transactions on Mobile Computing*, 2020.
- [3] T. Nitsche, C. Cordeiro, A. B. Flores, E. W. Knightly, E. Perahia, and J. C. Widmer, "IEEE 802.11ad: directional 60 GHz communication for multi-gigabit-per-second WiFi," in *IEEE Communications Magazine*, 2014.
- [4] Y. Ghasempour, C. R. Da Silva, C. Cordeiro, and E. W. Knightly, "IEEE 802.11ay: next-generation 60 GHz communication for 100 Gbps Wi-Fi," in *IEEE Communications Magazine*, 2017.
- [5] J. Lee, G. T. Gil, and Y. H. Lee, "Exploiting spatial sparsity for estimating channels of hybrid MIMO systems in millimeter wave communications," in *Proceedings of IEEE GLOBECOM*, 2014.
- [6] S. Payami, M. Shariat, M. Ghoraishi, and M. Dianati, "Effective RF codebook design and channel estimation for millimeter wave communication systems," in *Proceedings of IEEE ICC*, 2015.
- [7] D. Zhu, J. Choi, and R. W. Heath, "Auxiliary beam pair enabled AoD and AoA estimation in closed-loop large-scale millimeter-wave MIMO system," in *IEEE Transactions on Wireless Communications*, 2017.
- [8] J. Wang, Z. Lan, C. Pyo, T. Baykas, C. S. Sum, M. A. Rahman, J. Gao, R. Funada, F. Kojima, H. Harada, and S. Kato, "Beam codebook based beamforming protocol for multi-Gbps millimeter-wave WPAN systems," in *IEEE Journal on Selected Areas in Communications*, 2009.
- [9] S. Hur, T. Kim, D. J. Love, J. V. Krogmeier, T. A. Thomas, and A. Ghosh, "Millimeter wave beamforming for wireless backhaul and access in small cell networks," in *IEEE Transactions on Communica*tions, 2013.
- [10] A. Alkhateeb, O. E. Ayach, G. Leus, and R. W. Heath, "Channel estimation and hybrid precoding for millimeter wave cellular systems," in *IEEE Journal of Selected Topics in Signal Processing*, 2014.
- [11] B. Gao, Z. Xiao, L. Su, Z. Chen, D. Jin, and L. Zeng, "Multi-device multi-path beamforming training for 60-GHz millimeter-wave communications," in *Proceedings of IEEE ICC*, 2015.
- [12] A. Alkhateeb, G. Leusz, and R. W. Heath, "Compressed sensing based multi-user millimeter wave systems: How many measurements are needed?," in *Proceedings of IEEE ICASSP*, 2015.
- [13] R. Mendez-Rial, C. Rusu, A. Alkhateeb, N. Gozalez-Prelcic, and R. W. Heath, "Hybrid MIMO architectures for millimeter wave communications: phase shifters or switches?," in *IEEE Access*, 2015.
- [14] Z. Marzi, D. Ramasamy, and U. Madhow, "Compressive channel estimation and tracking for large arrays in mmwave picocells," in *IEEE Journal of Selected Topics in Signal Processing*, 2016.
- [15] O. Abari, H. Hassanieh, M. Rodreguez, and D. Katabi, "Millimeter wave communications: from point-to-point links to agile network connections," in *Proceedings of ACM HOTNETS*, 2016.
- [16] J. Mo and J. Walrand, "Fair end-to-end window-based congestion control," in *IEEE/ACM Transactions on Networking*, 2000.
- [17] C. Joe-Wong, S. Sen, T. Lan, and M. Chiang, "Multi-resource allocation: Fairness-efficiency tradeoffs in a unifying framework," in *IEEE/ACM Transactions on Networking*, 2013.
- [18] E. Aryafar and A. Keshavarz-Haddad, "Distributed alpha-fair throughput aggregation in multi-RAT wireless networks," in *Proceedings of IEEE WiOpt*, 2020.
- [19] S. Sur, I. Pefkianakis, X. Zhang, and K.-H. Kim, "WiFi assisted 60 GHz wireless networks," in *Proceedings of ACM MOBICOM*, 2017.
- [20] T. Nitsche, A. B. Flores, E. W. Knightly, and J. Widmer, "Steering with eyes closed: mm-wave beam steering without in-band measurement," in *Proceedings of IEEE INFOCOM*, 2015.
- [21] T. Wei, A. Zhou, and X. Zhang, "Facilitating robust 60 GHz network deployment by sensing ambient reflectors," in *Proceedings of USENIX* NSDI, 2017.
- [22] A. Zhou, X. Zhang, and H. Ma, "Beam-forecast: facilitating mobile 60 GHz networks via model-driven beam steering," in *Proceedings of IEEE INFOCOM*, 2017.
- [23] S. Sur, X. Zhang, P. Ramanathan, and R. Chandra, "Beamspy: enabling robust 60 GHz links under blockage," in *Proceedings of USENIX NSDI*, 2016.

- [24] A. Zhou, L. Wu, S. Xu, H. Ma, T. We, and X. Zhang, "Following the shadow: agile 3-D beam-steering for 60 GHz wireless networks," in Proceedings of IEEE INFOCOM, 2018.
- [25] M. Rakesh, Z. Marzi, Y. Zhu, U. Madhow, and H. Zheng, "Noncoherent mmwave path tracking," in *Proceedings of ACM HOTMOBILE*, 2017.
- [26] D. Steinmetzer, D. Wegemer, M. Schulz, J. Widmer, and M. Hollik, "Compressive millimeter-wave sector selection in off-the-shelf IEEE 802.11ad devices," in *Proceedings of ACM CONEXT*, 2017.
- [27] "Nexmon: the c-based firmware patching framework," Available at: https://nexmon.org.
- [28] A. Kochut, A. Vasan, A. U. Shankar, and A. Agrawala, "Sniffing out the correct physical layer capture model in 802.11b," in *Proceedings of IEEE ICNP*, 2004.
- [29] "Uplink power control in Ite," https://www.qualcomm.com/videos/uplink-power-control-Ite.
- [30] 3GPP TS 36.213, "E-UTRA physical layer procedure," 2020.
- [31] 3GPP TR 38.901, "Study on channel model for frequencies from 0.5 to 100 GHz," 2019.